



Incompressible Turbulent Flow Reconstruction by the POD technique

Juan d'Adamo, Guillermo Artana, Jean-Antoine Desideri

► To cite this version:

Juan d'Adamo, Guillermo Artana, Jean-Antoine Desideri. Incompressible Turbulent Flow Reconstruction by the POD technique. [Research Report] RR-5278, INRIA. 2004, pp.21. inria-00070722

HAL Id: inria-00070722

<https://hal.inria.fr/inria-00070722>

Submitted on 19 May 2006

HAL is a multi-disciplinary open access archive for the deposit and dissemination of scientific research documents, whether they are published or not. The documents may come from teaching and research institutions in France or abroad, or from public or private research centers.

L'archive ouverte pluridisciplinaire **HAL**, est destinée au dépôt et à la diffusion de documents scientifiques de niveau recherche, publiés ou non, émanant des établissements d'enseignement et de recherche français ou étrangers, des laboratoires publics ou privés.

Incompressible Turbulent Flow Reconstruction by the POD technique

Juan D'Adamo — Guillermo Artana — Jean-Antoine Désidéri

N° 5278

July 2004

Thème NUM



*rapport
de recherche*

Incompressible Turbulent Flow Reconstruction by the POD technique

Juan D'Adamo ^{*}, Guillermo Artana ^{*}, Jean-Antoine Désidéri[†]

Thème NUM — Systèmes numériques
Projet Opale

Rapport de recherche n° 5278 — July 2004 — 21 pages

Abstract: With this work, we intend to achieve reduced dynamical models for an incompressible turbulent external flow. The model is constructed from a set of particle image velocimetry [6] (PIV) measurements, using the velocity field data obtained in previous experiments [10]. The Proper Orthogonal Decomposition (POD) is as a technique which allows the extraction of the significant modes of a flow. It permits to identify modes without any a priori hypothesis, and these are ordered by their associated level of energy. The POD modes are used to formulate a dynamical system which only contains the main features of the flow, a low order dynamical system (LODS). This is achieved by means of a Galerkin projection of the Navier-Stokes Equations with the goal to obtain a system of ordinary differential equations describing the main aspects of the flow without demanding excessive computational requirements.

Key-words: POD, PIV, low order dynamical systems, turbulence, incompressible flow

^{*} Laboratorio de Fluidodinámica Universidad de Buenos Aires

[†] INRIA Sophia Antipolis

Reconstruction d'un écoulement incompressible turbulent par la technique POD

Résumé : Dans ce travail, nous nous proposons d'étudier des modèles dynamiques réduits pour un écoulement incompressible, turbulent et externe. Le modèle se génère à partir d'un ensemble de mesures de vélocimétrie par images de particules (PIV). La méthode de décomposition aux valeurs propres (POD) est une technique qui réalise l'extraction des modes principaux d'un écoulement. Elle permet l'identification de ces modes sans hypothèses a priori, et ils sont ordonnés par leur niveau d'énergie associé. Les modes obtenus par la méthode POD sont utilisés pour la formulation d'un système dynamique d'ordre bas (LODS) contenant uniquement les caractéristiques essentielles de l'écoulement. On termine par une projection de Galerkin des équations de Navier-Stokes, dans le but d'obtenir un système d'équations différentielles ordinaires, qui puisse décrire les aspects principaux de l'écoulement sans nécessiter de ressources informatiques excessives.

Mots-clés : Vélocimétrie par Images de Particules (PIV), Proper Orthogonale Decomposition (POD) ou Décomposition aux valeurs propres, systèmes dynamiques d'ordre bas, turbulence, écoulements incompressibles

Contents

| | | |
|----------|--|-----------|
| 1 | Introduction | 4 |
| 1.1 | Identification of coherent structures: the Proper Orthogonal Decomposition (POD) | 4 |
| 1.2 | Formulation of the low order dynamic system (LODS) POD- Galerkin projection | 6 |
| 2 | The experimental data | 7 |
| 3 | Problem Description | 8 |
| 4 | Results | 8 |
| 5 | Conclusions | 9 |
| 6 | Figures | 11 |

1 Introduction

The reduction of the Navier-Stokes equations to a system of ordinary differential equations (ODE) has been largely studied by the Computational Fluid Dynamics (CFD) community. With different tools developed in this domain, it has been possible to reproduce or predict diverse flow characteristics with a large detail. The computational cost of these calculations becomes higher as the Reynolds number increases and when turbulent models must be adopted.

For these reasons, different research efforts have been made in the literature to deal with viscous turbulent flows but with a less ambitious goal consisting of treating low dimensional dynamic models (LODS) or reduced order models. These capture just the essential characteristics, coherent structures of the flow and their dynamics, sacrificing its detailed structures.

Some scenarios where these models are of interest are in flow control applications where simple systems are required. Actuation on coherent structures may be largely amplified, producing important modifications of the flow characteristics (boundary layer separation, vortex shedding, ...).

Also in shape optimization problems, it is of interest to avoid the repetition of CFD calculations, working with LODS would accelerate the tasks.

Lastly, LODS can be helpful in experimental fluid mechanics where it is required to improve the temporal resolution of flow fields measurements obtained with Particle Image Velocimetry techniques.

A way to obtain LODS is by means of the Proper Orthogonal Decomposition technique, that allows to extract a set of basis functions onto which the flow equations are projected. Unlike classical CFD, POD formulation requires to know a set of the flow fields issued from direct simulation databases: we can mention in this respect the works of Rajaei (1994)[7] Ravindran (2002)[8], and, in compressible-flow applications, closely related to numerical developments at INRIA: Iollo (1998)[5] and Vigo (2000)[11]. By other hand, the POD method has been also applied to experimental data, and particularly PIV. In this sense, Braud (2003)[1] has used it to analyse the dynamics of a mixing layer - wake interaction.

1.1 Identification of coherent structures: the Proper Orthogonal Decomposition (POD)

The Proper Orthogonal Decomposition (POD) was first introduced in the context of turbulence by Lumley (1967). It has been used by different authors (for a complete review see for instance Holmes (1996)[3]) as a technique to obtain approximate descriptions of the large scale or coherent structures in laminar and turbulent flows.

Given an ensemble $\vec{u}(\vec{x}, t_i)$ obtained experimentally, belonging to M discrete times, POD provides M basic functions $\vec{\phi}_i(x)$, which are optimal with respect to the ability of represent-

ing the kinetic energy of the flux. The aim of the decomposition is to write

$$\vec{u}(\vec{x}, t) = \sum_{i=1}^M a_i(t) \vec{\phi}_i(\vec{x}) \quad (1)$$

We denote by (\cdot, \cdot) the inner product of vector fields defined in $L^2(S)$ where S represents the spatial domain occupied by the flux. So that,

$$(\vec{u}, \vec{\phi}) = \iint_S \vec{u} \cdot \vec{\phi} ds$$

We seek a subspace such that the projection of $\vec{u}(\vec{x}, t_i)$ onto it is optimal along the sampling time.

Then the problem is to find an ensemble of functions that maximizes:

$$\frac{\langle |(\vec{u}, \vec{\phi})|^2 \rangle}{|(\vec{\phi}, \vec{\phi})|^{1/2}}$$

where $\langle \bullet \rangle$ denotes a temporal average. It can be demonstrated [see for example Holmes [3]] that the maximization problem leads to the following eigenvalue problem:

$$\iint_S R(\vec{x}, \vec{x}') \vec{\phi}_k(\vec{x}) ds = \vec{\phi}_k(\vec{x}) \lambda_k \quad (2)$$

Where R is the spatial correlation matrix $R(\vec{x}) = \int \vec{u}(\vec{x}, t) \vec{u}(\vec{x}', t) dt$

One POD property is that each eigenvalue λ_k quantifies the kinetic energy of the ϕ_k mode. Following Sirovich [9] Snapshots method (1987), the spatial modes can be built from a suitable superposition of the velocities,

$$\vec{\phi}_k(\vec{x}) = \sum_{i=1}^n a_i(t) \vec{u}(\vec{x}, t) \quad (3)$$

Injecting the latter equation into (2) we arrive at the following eigenvalue problem

$$Ca = \lambda a$$

where

$$C(t, t') = \frac{1}{M} \iint_S \vec{u}(\vec{x}, t) \vec{u}(\vec{x}, t') ds$$

It is verified that this tensor is symmetric and semi-positive definite. Then, it is possible to obtain the temporal modes $a_i(t)$ of the decomposition as the components of the $k - th$ eigenvector of the temporal correlation matrix C , where $\langle a_k, a_l \rangle = \lambda_k \delta_{kl}$.

And these λ_k 's are also the solution of (2) but associated with other eigenvectors. Once the $a_i(t)$'s calculated, the solution for the spatial modes $\vec{\phi}_i$ is immediate using equation (3).

1.2 Formulation of the low order dynamic system (LODS) POD- Galerkin projection

From the modal decomposition, it is possible to consider a truncated model accounting for s modes to approximate the velocity field $\vec{u}(\vec{x}, t_i)$, with $\vec{x} \in S$, $1 \leq i \leq M$, $s \ll M$. The percentage energy contained in this model will be

$$\frac{\sum_{i=1}^s \lambda_i}{\sum_{i=1}^M \lambda_i}$$

A method to convert a partial differential equation (PDE) system in a system of ordinary differential equation (ODE) is the Galerkin projection. According to this procedure, the functions which define the original equations are projected on a finite dimensional subspace of the phase space (in this case, the subspace generated by the first s modes). To avoid pressure terms, we have dealt with the vorticity equation:

$$\frac{D\vec{\Omega}}{Dt} + \vec{grad}(\vec{\Omega})\vec{u} = \vec{grad}(\vec{u})\vec{\Omega} + \nu \Delta \vec{\Omega} \quad (4)$$

For a turbulent case, we apply the Reynolds decomposition. The vorticity equation can be written in terms of a mean value and a fluctuation of the velocity \vec{u} and the vorticity $\vec{\Omega}$.

$$\vec{u} = \vec{u}_m + \vec{\tilde{u}} \text{ and } \vec{\Omega} = \vec{\Omega}_m + \vec{\tilde{\Omega}}$$

$$\begin{aligned} \frac{\partial \vec{\tilde{\Omega}}}{\partial t} + \vec{grad}(\vec{\tilde{\Omega}})\vec{\tilde{u}} - (\vec{grad}(\vec{\tilde{\Omega}})\vec{\tilde{u}})_m + \vec{grad}(\vec{\Omega}_m)\vec{\tilde{u}} + \vec{grad}(\vec{\tilde{\Omega}})\vec{u}_m = \\ \vec{grad}(\vec{\tilde{u}})\vec{\tilde{\Omega}} - (\vec{grad}(\vec{\tilde{u}})\vec{\tilde{\Omega}})_m + \vec{grad}(\vec{\tilde{u}})\vec{\Omega}_m + \vec{grad}(\vec{u}_m)\vec{\tilde{\Omega}} + \frac{2}{Re} \Delta \vec{\tilde{\Omega}} \end{aligned} \quad (5)$$

The projection of the latter equation on the subspace generated by the ϕ_k modes ($k \in [1 \dots s]$) leads us to a system of ODE of order 1 with quadratic terms.

This system is solved starting for some initial condition, to compute the projection of the velocity fields into the first s modes. The solutions of this system are the temporal modes $a_k(t)$:

$$M\dot{a} = La + \hat{a}^T C \hat{a} + I_{dp} \quad (6)$$

$$\text{where } M(i, j) = \iint_S \vec{\psi}_i \vec{\psi}_j ds \quad \vec{\psi} = \text{rot}(\vec{\phi})$$

$$L(i, j) = \frac{2}{Re} \iint_S \Delta \vec{\psi}_i \vec{\psi}_j ds - \iint_S (\vec{\phi}_i \nabla \vec{\Omega}_m + \vec{u}_m \nabla \vec{\psi}_i) \cdot \vec{\psi}_j ds$$

$$C = \begin{pmatrix} C_1 & 0 & 0 & 0 & \dots \\ 0 & C_2 & 0 & 0 & \dots \\ 0 & 0 & \dots & 0 & \dots \\ 0 & 0 & 0 & \dots & \dots \\ 0 & 0 & 0 & 0 & C_s \end{pmatrix}$$

with each $C(i, j)_k = -\iint_S (\nabla \vec{\psi}_i \vec{\phi}_j) \cdot \vec{\psi}_k ds$

$$I_{dp}(k) = (\lambda_1 \dots \lambda_S) \cdot \text{diag}(C_k)$$

$$\hat{a} = \begin{pmatrix} a \\ a \\ \dots \\ \dots \\ a \end{pmatrix} \text{ } s \text{ times.}$$

To calculate the derivatives we followed Rajaei and Sirovich's scheme [7], in order to minimize numerical errors due to discretisation. The integrals were evaluated by the trapezoidal method. The resolution of the system (6) was done with a Runge-Kutta 4th order method.

2 The experimental data

Particle Image Velocimetry (PIV) is a recent measurement technique that allows to determine a set of instantaneous velocity fields in large regions (see for instance Keane and Adrian (1992)[6]. It is non intrusive, being based on optical acquisition and image processing methods.

Particle tracers (seeders) are injected into the flow and with suitable illumination, they diffuse the light towards sensitive cameras. From correlations of pairs of images, tracers' paths are estimated as well as the flow velocity field is. Time-depend behaviour of flows can be studied in spite of a technical limitation: the time distance between each pair of images is, at best, of the order of 1/3 second.

At present, PIV is commonly used for CFD validation in many domains. Though still mainly limited for low Mach numbers applications, the method is constantly improved (for example Hart(2000)[2]) and makes PIV a very promising technique.

The measurements were done in a wind tunnel loop of the Laboratoire d'Etudes Aérodynamiques of Université de Potiers. The tunnel has a rectangular cross section (0.50 x 0.50 m²) and enables testing at flow velocities up to 30 m/s. The NACA 0015 chord dimension was 200 mm and the spanwise dimension was 450 mm. The velocity field was measured using a Particle Image Velocimetry (PIV) technique. Treatment of the recorded images was undertaken with commercial PIV software enabling the use of an adaptive correlation technique to obtain the vector fields. In this treatment, two refinements steps were considered

and the final interrogation area size was of 16×16 pixels² with an overlap of 50%. Three hundred pairs of digital images taken at pairs every 0.1s were examined in each experiment. For further details on the experimental setup see Sosa (2004)[10].

3 Problem Description

We studied the flow around an airfoil NACA 0015 at high angles of attack ($\alpha > 15^\circ$), for Reynolds numbers between 150000 and 333000. The flow regime is turbulent though characterized by an almost coherent vortex shedding, as pointed out by Huang (1995)[4] for a similar case.

The Strouhal number, $St = \frac{fL_c}{U}$, referred to the chord dimension L_c is of the order of 0.2. This means that the range of frequencies of vortex shedding is about tenths of Hz. The time sampling results then insufficient to follow the flow dynamics. However this problem can be sorted out, at least for the large structures, by means of the POD-Galerkin method.

4 Results

For a flow with an angle of attack $\alpha = 19.9^\circ$, $Re = 333000$, see Figure 1 for a typical velocity field, we applied the POD method. We found the kinetic energy distribution for the fluctuant velocity field, represented by the eigenvalues λ_k in Figure 2.

It can be observed that 41% of the fluctuant kinetic energy is contained in 15 modes. Further modes would make a dynamical system of more than 15 differential equations, with its associated numerical problems. Though it doesn't reach the high values as in CFD data decompositions (usually up to 90%), it is enough to reconstruct the large structures. A way to show this is to compare a spatial correlation reconstructed and measured, as made by Braud [1].

Figure 3 illustrates the spatial correlation with respect a point (x_a, y_a) at the vortex shedding region for the truncated model and for the measured flow. It is observed that the correlation reveals more detailed structures at the flow measured (300 modes) than at the truncated modes flow. However, it is clear that the large scales are retained.

In figure 4, the mean flow, statistically stationary, represents the largest scale of the flow. The topology of the spatial modes shows the vortex structures. They are ordered by POD from the most energetic, great scale structures, ϕ_1 in Figure 5, to the smaller ones (for example ϕ_5 in Figure 6). Because of the spatial resolution, the smallest scales of the flow i.e., the shear layer vortex shedding, cannot be resolved.

To solve the dynamical system, we utilised a fourth order Runge-Kutta scheme, which is standard for Galerkin method applied to convection-dominated flow. The direct application of the Runge-Kutta scheme to Equation (6) results in an unstable numerical simulation.

From a numerical point of view, we analysed the system stability by studying its behaviour under 2 regimes: Stokes flow and Pure convection. In the first case, we confirmed that our system converges to the trivial solution when $Re \sim 1$. The second case, a non-viscous flow, diverges too soon, due to a spatial numerical instability. In consequence, we decided to introduce an artificial viscosity term to stabilize the system.

On the other hand, from a physical point of view, the system lacks of terms of dissipation, being the linear viscous term smaller than the others. The turbulent dissipation is mainly due to the scales unresolved by the system. Then, according to Holmes [3], we adjusted a term for the turbulent dissipation in function of the resolved modes: $-\alpha\nu_T\Delta\tilde{\Omega}$. In other words, we have added the linear term

$$L_v(i, j) = \frac{\nu_T}{UL} \iint_S \Delta\psi_i\psi_j ds$$

Then the dynamic system becomes the following:

$$M\dot{a} = (L + L_v)a + \hat{a}^T C \hat{a} + I_{dp} \quad (7)$$

With a value of ν_T around $2.9 \cdot 10^{-3}$, 200 times the kinematic viscosity, the solution was then stable and periodic. We have observed a great sensitivity of the method to the value of the coefficient α . For $\alpha < 0.98$, the numerical system is unstable. For $\alpha > 1.03$, the system goes to zero trivially. We have used $\alpha = 1$.

In this way, the values $a_i(t)$, unavailable experimentally are obtained. The reconstruction of the flow by the reduced order model is immediate by:

$$\vec{u}_{reconstructed}(\vec{x}, t) = \vec{u}_m + \sum_{i=1}^s a_i(t) \vec{\phi}_i(\vec{x})$$

Figure 7 shows the continuous solution for three modes $a_i(t)$ in comparison with the discrete data $a_i(t_i)$ corresponding to each snapshot. Near the initial condition, the numerical solution is very close to the first discrete data points.

A dominant frequency can be extracted from the spectral analysis of the solutions, as displayed in Figure 8. The dominant frequency is about 40 Hz, a value around the expected magnitude that corresponds to the main vortex shedding.

A phase diagram (Figure 9) points out the system attractor for a particular initial condition. The solutions take the form of a limit cycle. They are also represented the cases of divergence (Figure 10) and convergence to a trivial solution (Figure 11).

5 Conclusions

We succeeded to model experimental PIV data for an incompressible turbulent flow around a NACA 0015 airfoil by means of the POD-Galerkin technique. The essential modes of the

flow were extracted and consequently a low order dynamical system was introduced. With 15 modes we were able to describe the main features of this flow.

A stable and periodic solution of the system was found when adding an artificial viscosity, which accounted for the dissipation of the turbulent stresses. Concerning the acquisition, at least for the great scales of the flow, we succeeded to follow dynamics that are out of PIV temporal resolution. Regarding the introduction of a turbulent stress, a more accurate model should be developed, to study the relationship between the solved and unresolved modes for this flow.

Lastly, future works could also benefit from this development in design optimization and flow control applications in similar configurations.

References

- [1] BRAUD Caroline. Etude de la dynamique d'un écoulement à cisaillements croisés : interaction couche de mélange - sillage. Thèse de doctorat (12 décembre 2003), Université de Poitiers.
- [2] HART D.P. Super-resolution PIV by recursive local-correlation. *Journal of Visualization*, 3(2):187-194, september 2000.
- [3] HOLMES, P. J., J. L. LUMLEY, and G. BERKOOZ. 1996. *Turbulence, coherent structures, symmetry and dynamical systems*. Cambridge, UK: Cambridge University Press.
- [4] HUANG Rong F., LIN Chih L., Vortex Shedding and Shear-Layer Instability of Wing at Low-Reynolds Numbers, *AIAA Journal*, Vol. 33, No.8, August 1995.
- [5] IOLLO A., LANTERI S., DESIDERI J.A., Stability Properties of POD-Galerkin Approximations for the COMPRESSIBLE NAVIER STOKES EQUATIONS, INRIA Research Rapport n° RR-3589, 1998
- [6] KEANE R., ADRIAN R., Theory of Cross Correlation Analysis of PIV Images", *Applied Scientific Research*, Vol 49, 1992 pp 191-215.
- [7] RAJAEE M, KARLSON SKF, SIROVICH L. Low-dimensional description of free shear flow coherent structures and their dynamical behavior. *Journal of Fluid Mechanics* 1994; 258: 1401-1402.
- [8] S.S. RAVINDRAN : Control of flow separation over a forward-facing step by Model reduction, *Computer Methods in Applied Mechanics and Engineering*, Vol 191, pp 4599-4617, 2002.
- [9] SIROVICH, L. (1987) Turbulence and the dynamics of coherent structures, Part I-III, *Quarterly of Appl. Math.*, XLV(3), pp. 561-82.
- [10] SOSA R., MOREAU E., TOUCHARD G., ARTANA G., Stall Control at High Angle of Attack with Periodically Excited EHD Actuators, *AIAA Paper* 2004-2738.

- [11] VIGO Guillaume, Méthodes de décomposition orthogonales aux valeurs propres appliquées aux écoulements instationnaires compressibles complexes, Thèse de doctorat (16 novembre 2000), Université PARIS IX DAUPHINE.

6 Figures

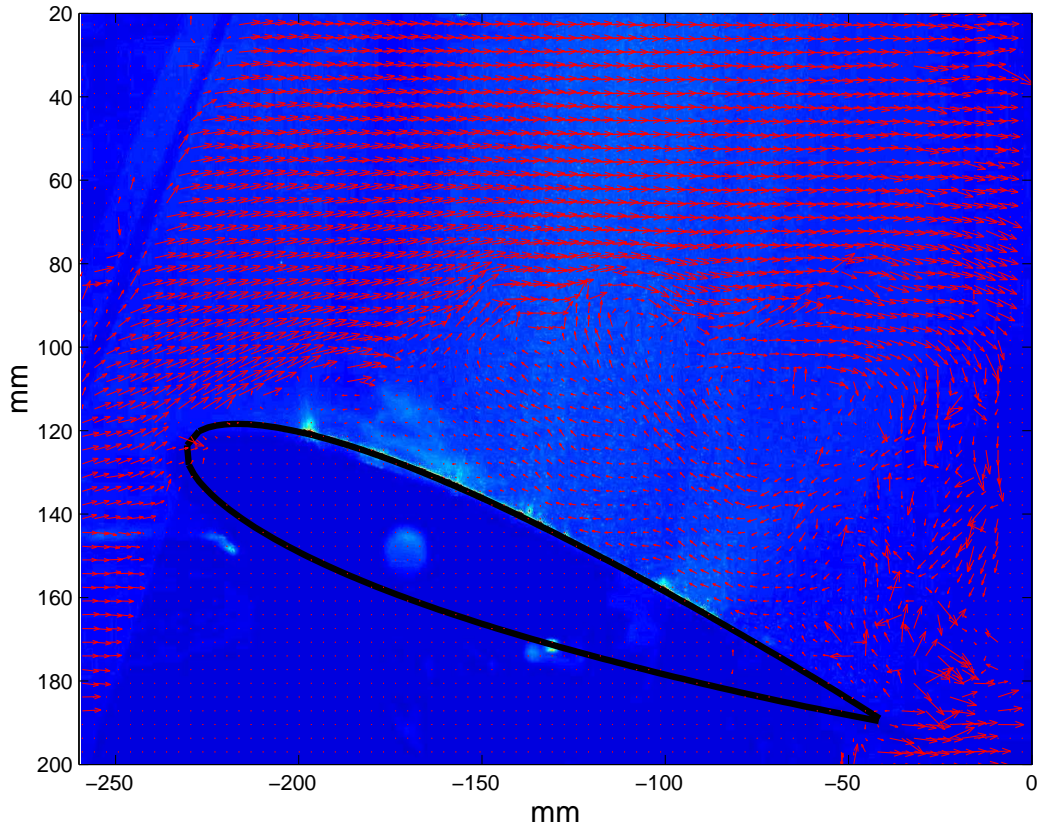


Figure 1: Typical Instantaneous PIV Flow Field. $\alpha = 19.9^\circ$ $Re = 333000$

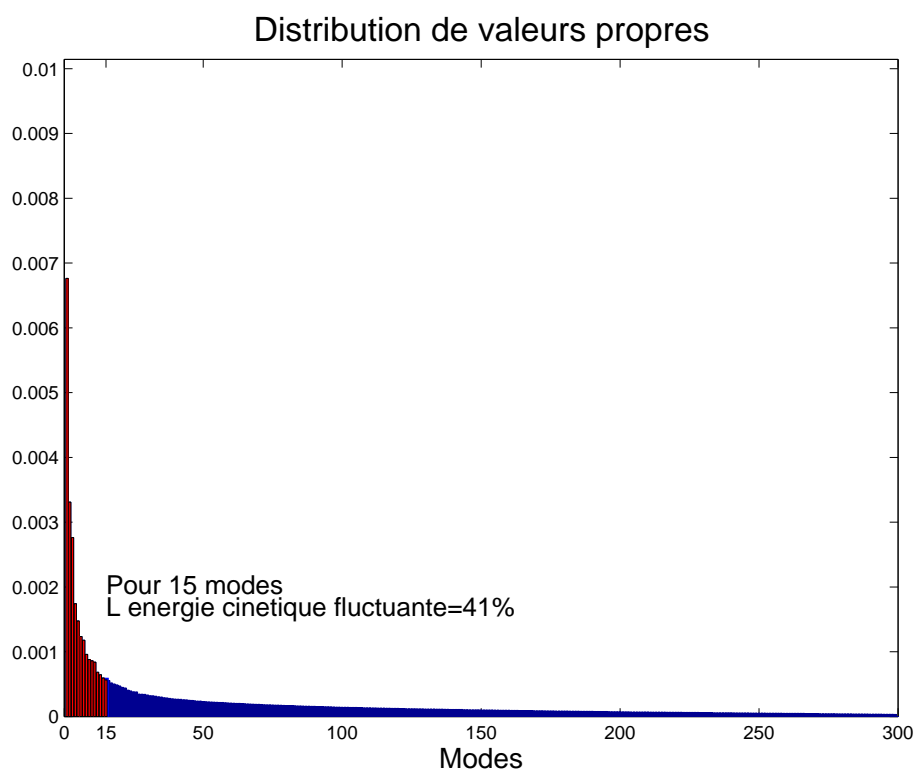


Figure 2: POD modes energy distribution

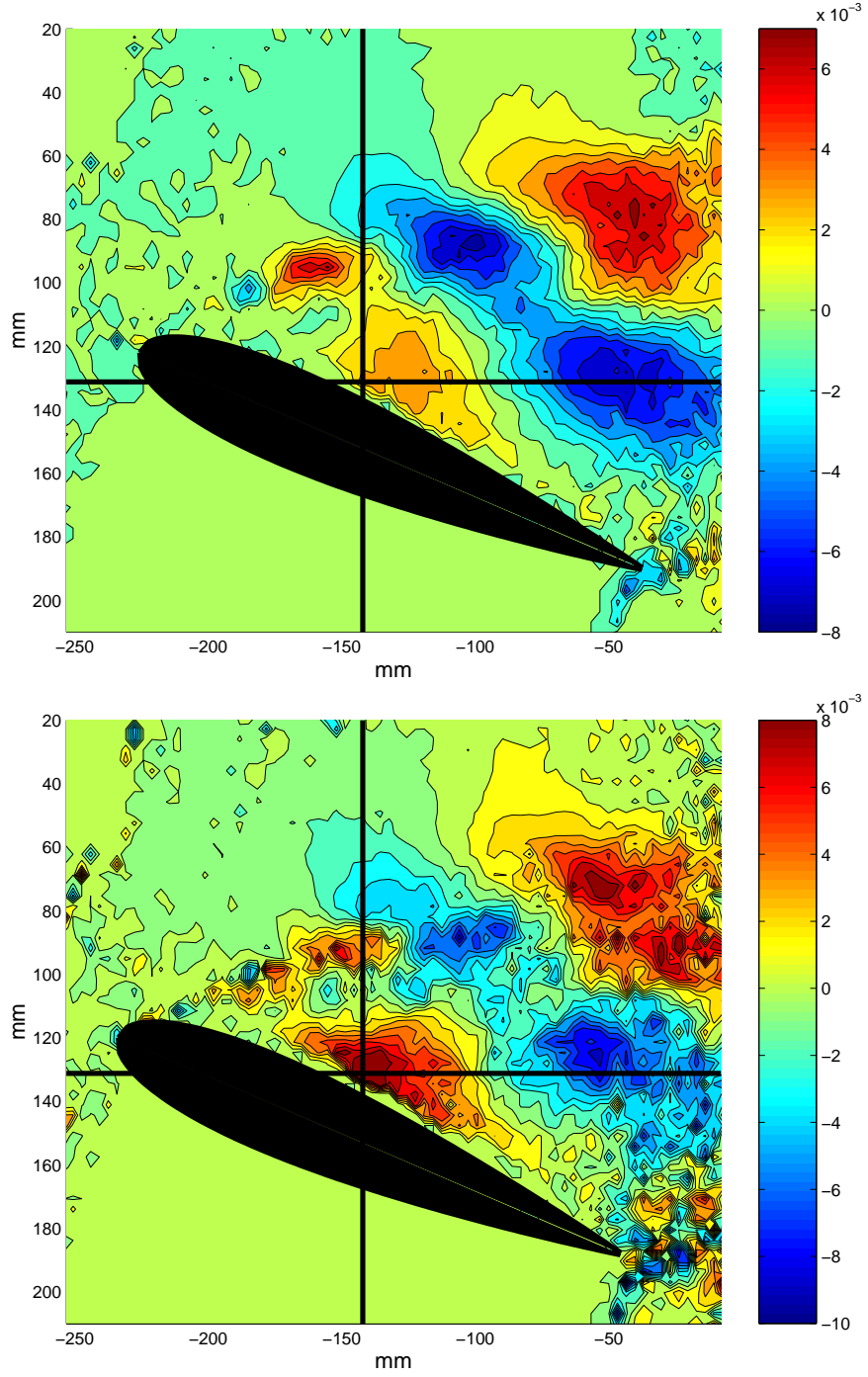


Figure 3: Spatial Correlation: a) 15 modes, b) 300 modes (total).

$$\sum_{i=1}^s \lambda_i \vec{\phi}(x, y) \vec{\phi}(x_a, y_a) \quad (x_a, y_a) = (-144, 131)$$

$$R(x, y, x_a, y_a) =$$

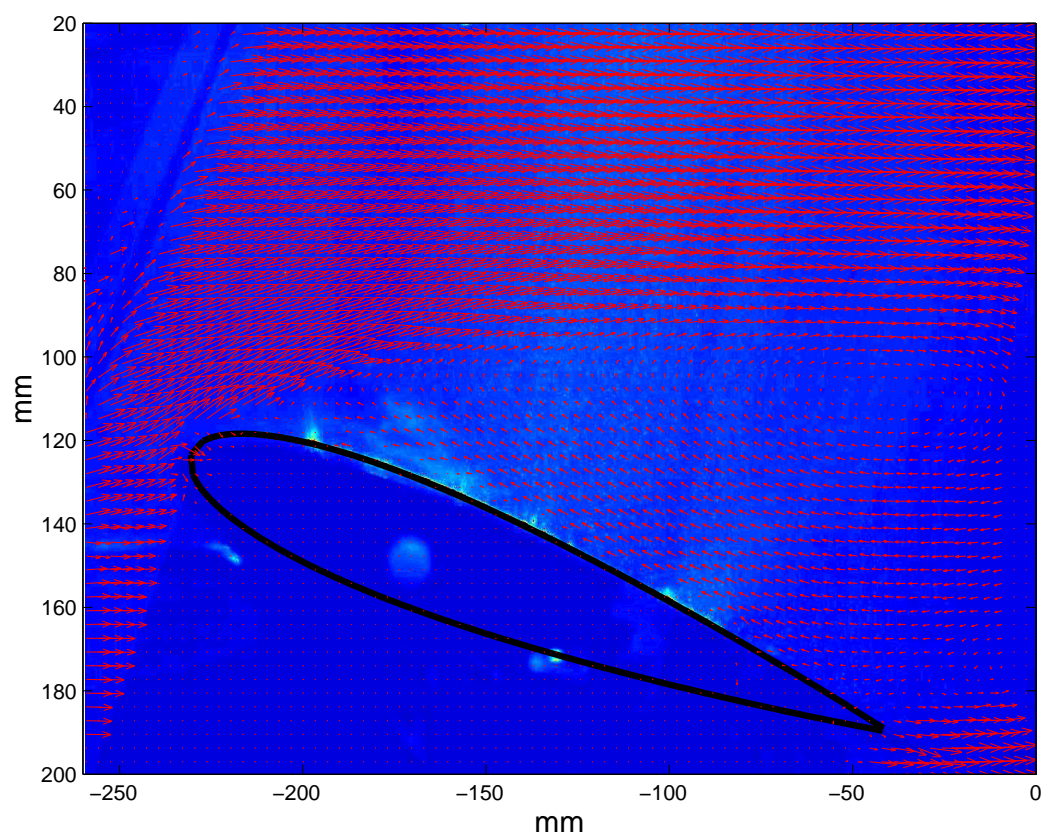


Figure 4: Mean Flow

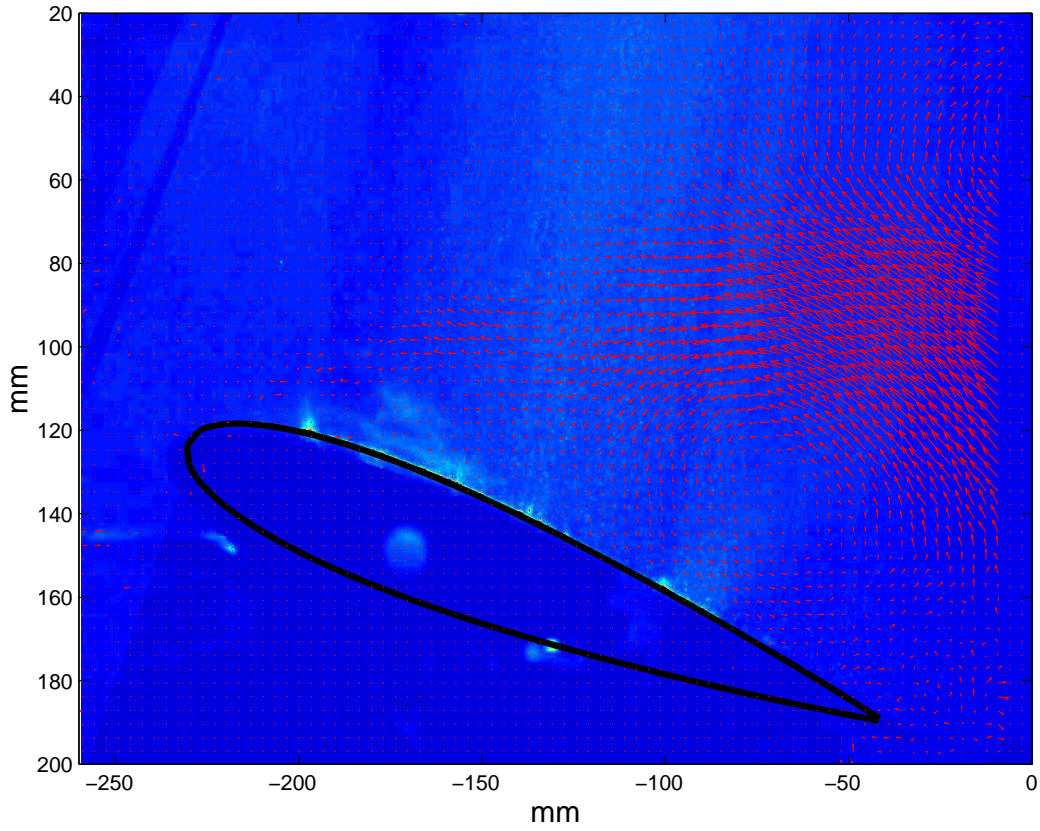


Figure 5: TOPOLOGY, Mode $\vec{\phi}_1(\vec{x})$

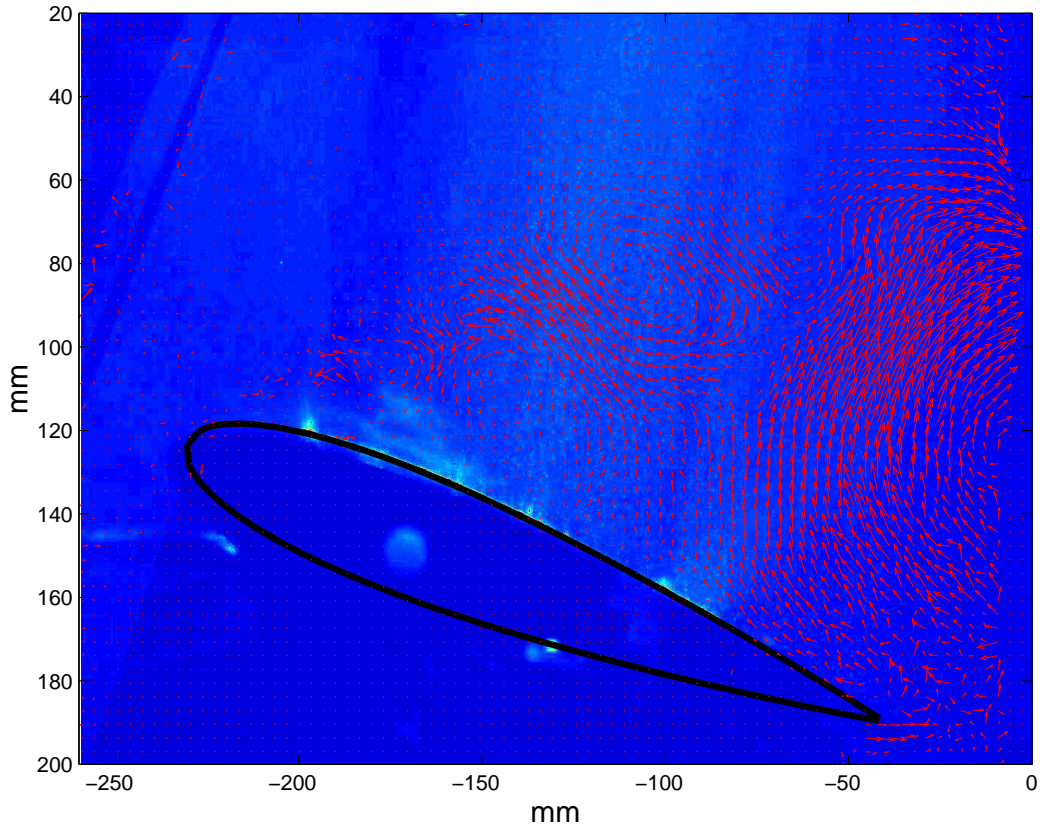


Figure 6: TOPOLOGY, Mode $\vec{\phi}_5(\vec{x})$

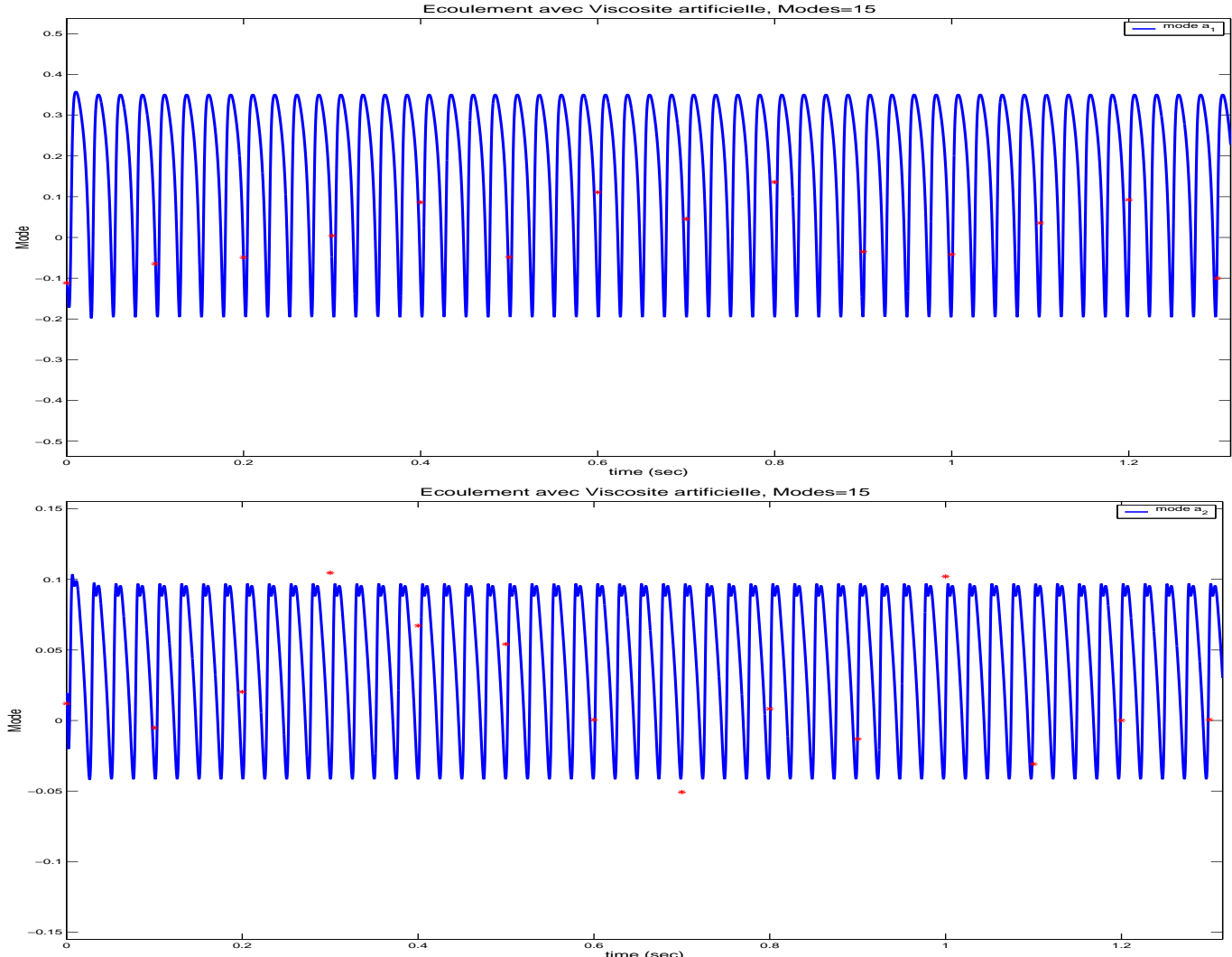


Figure 7: Solutions of the dynamical system: a) $a_1(t)$ and $a_1(t_i)$, b) $a_2(t)$ and $a_2(t_i)$

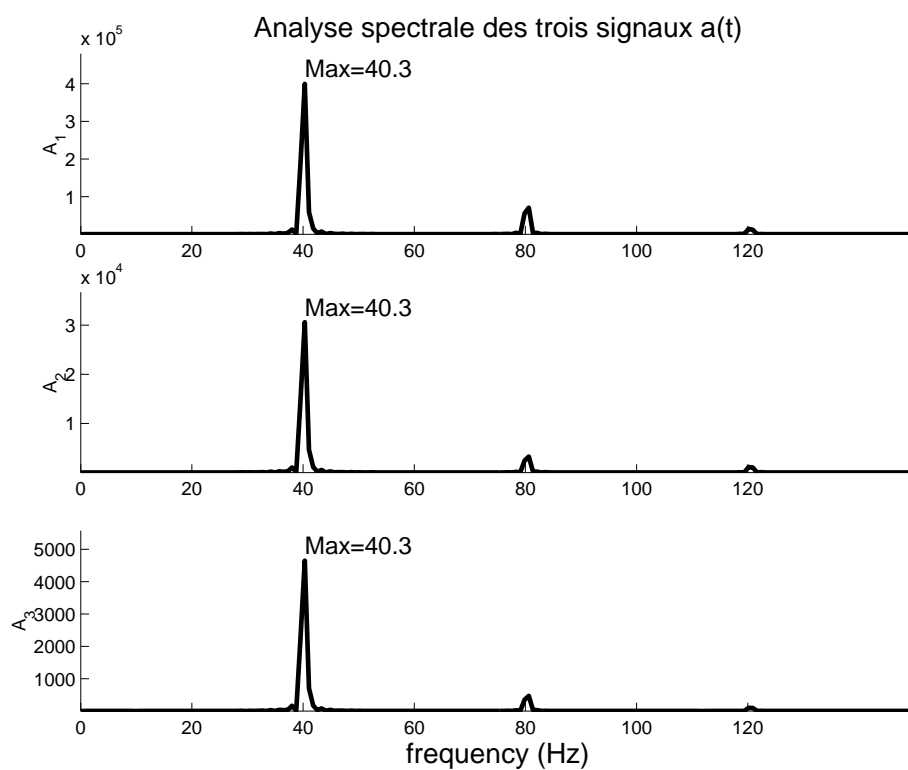


Figure 8: Spectral distribution of the first 3 modes

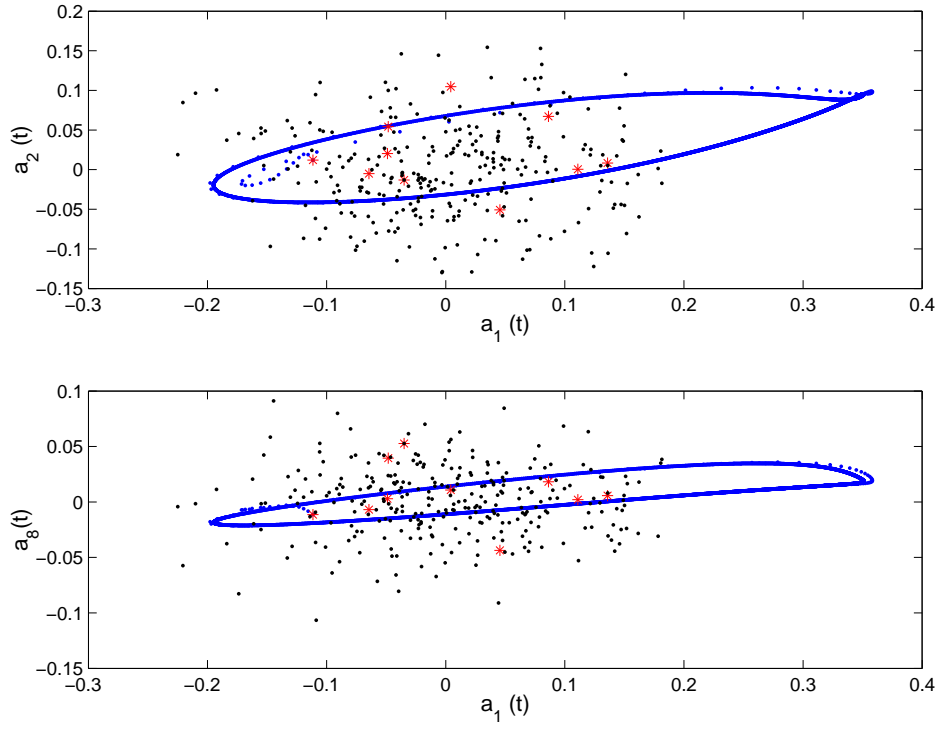


Figure 9: Stable Solution $\alpha = 1$. Phases Portraits $a_1(t)$ vs $a_2(t)$; $a_1(t)$ vs $a_8(t)$. Discrete points are also represented, those near the initial condition (red) and the others (black).

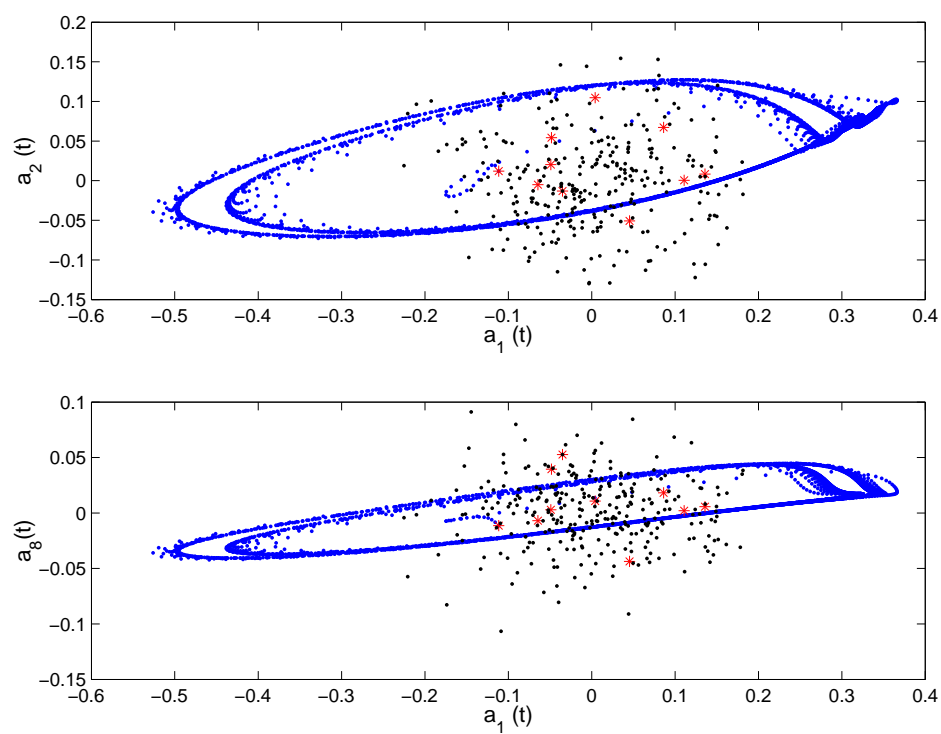


Figure 10: Divergent Solution $\alpha < 0.98$. Phases Portraits $a_1(t)$ vs $a_2(t)$; $a_1(t)$ vs $a_8(t)$.

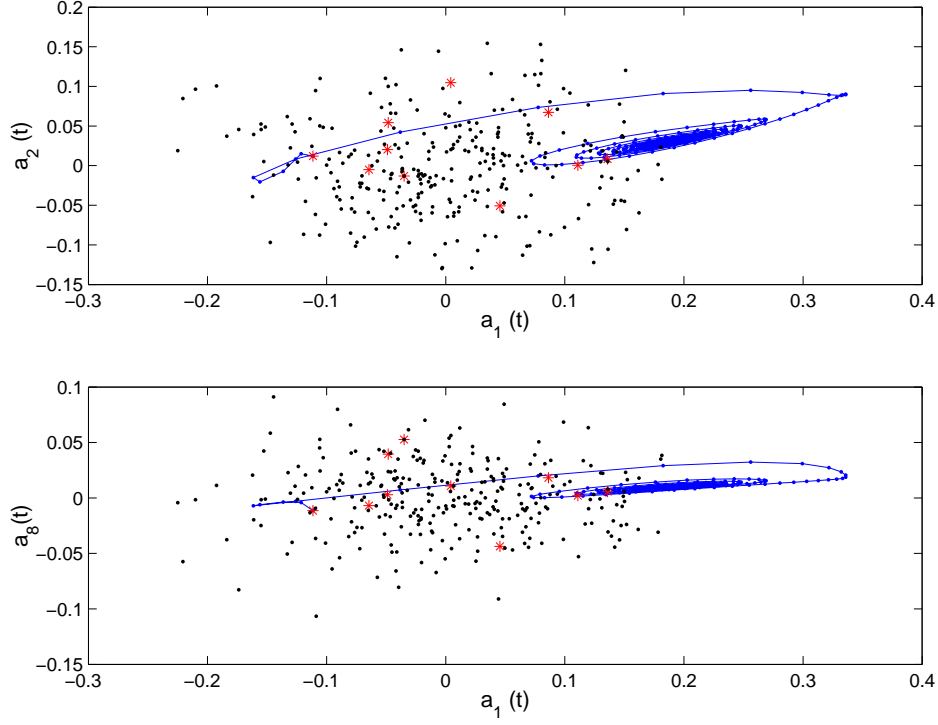


Figure 11: Convergent Trivial Solution $\alpha > 1.03$. Phases Portraits $a_1(t)$ vs $a_2(t)$; $a_1(t)$ vs $a_8(t)$.



Unité de recherche INRIA Sophia Antipolis
2004, route des Lucioles - BP 93 - 06902 Sophia Antipolis Cedex (France)

Unité de recherche INRIA Futurs : Parc Club Orsay Université - ZAC des Vignes
4, rue Jacques Monod - 91893 ORSAY Cedex (France)

Unité de recherche INRIA Lorraine : LORIA, Technopôle de Nancy-Brabois - Campus scientifique
615, rue du Jardin Botanique - BP 101 - 54602 Villers-lès-Nancy Cedex (France)

Unité de recherche INRIA Rennes : IRISA, Campus universitaire de Beaulieu - 35042 Rennes Cedex (France)

Unité de recherche INRIA Rhône-Alpes : 655, avenue de l'Europe - 38334 Montbonnot Saint-Ismier (France)

Unité de recherche INRIA Rocquencourt : Domaine de Voluceau - Rocquencourt - BP 105 - 78153 Le Chesnay Cedex (France)

Éditeur
INRIA - Domaine de Voluceau - Rocquencourt, BP 105 - 78153 Le Chesnay Cedex (France)
<http://www.inria.fr>
ISSN 0249-6399